THE ASTROPHYSICAL JOURNAL, 394:581–585, 1992 August 1

ROTATIONAL PARAMETERS OF PSR 0540−69 AS MEASURED AT OPTICAL WAVELENGTHS

CHRISTIAN GOUIFFES
European Southern Observatory, Karl-Schwarzschild-Straße 2, D-8046 Garching, Federal Republic of Germany
JOHN P. FINLEY
Department of Physics, University of Wisconsin-Madison, 1150 University Avenue, Madison, WI 53706
AND
HAKKI ÖGELMAN
Department of Physics, University of Wisconsin-Madison, 1150 University Avenue, Madison, WI 53706, and Max-Planck-Institut für Extraterrestrische Physik, Karl-Schwarzschild-Straße 1, D-8046 Garching, Federal Republic of Germany
Received 1991 November 18; accepted 1992 February 10

ABSTRACT

We have measured the rotation frequency of the 50 ms pulsar PSR 0540−69 utilizing data collected at the ESO 3.6 m telescope at La Silla. The observations were acquired in the interval 1989 January–1991 April. The average pulse shape displays a broad enhancement with a superposed double-peaked structure. We were able to phase-relate the data between 1990 March and 1991 April indicating the pulsar did not display any large spin discontinuities during that time span. Three solutions, incorporating a pulse number ambiguity of ± 1, are presented. Our preferred solution yields a braking index of 2.04 ± 0.02, comparable with *GINGA* measurements in 1987. Discrepancies between our results and extrapolation of the *GINGA* results are discussed.

Subject headings: pulsars: individual (PSR 0540−69) — stars: rotation

1. INTRODUCTION

PSR 0540−69 is a 50 ms pulsar in the Large Magellanic Cloud (LMC) discovered in the soft X-ray band by the *Einstein* satellite in 1984 (Seward, Harnden, & Helfand 1984). Optical pulsations from the source were subsequently observed in 1985 (Middleditch & Pennypacker 1985). The energetics, age, and morphology of PSR 0540−69 are similar to those of the Crab pulsar. Owing to its large distance of ~55 kpc, however, it has not been possible to observe PSR 0540−69 at radio frequencies. For this reason frequency measurements which can yield a $\ddot{\nu}$ and a braking index must rely on an orbiting X-ray satellite or a large optical telescope capable of detecting the 23 mag pulsations. To date, measurements of $\ddot{\nu}$ have come from a combination of (*a*) *Einstein* + CTIO data (Middleditch, Pennypacker, & Burns 1985), (*b*) CTIO + *Einstein* + *EXOSAT* data (Ögelman & Hasinger 1990), (*c*) *GINGA* data (Nagase et al. 1990), and (*d*) the Anglo-Australian Telescope (AAT) (Manchester & Peterson 1989). The braking index measurement of Ögelman & Hasinger (1990), $n = 2.74 \pm 0.10$, utilizing *Einstein*, *EXOSAT*, and CTIO data contemporaneous with the X-ray data was found to be incompatible with the *GINGA* and AAT measurements, $n = 2.04 \pm 0.01$ and $n = 2.01 \pm 0.02$, respectively, which commenced approximately 1 yr after the *EXOSAT* mission. Ögelman & Hasinger (1990) concluded that PSR 0540−69 may be a pulsar which displays significant discontinuities in its spin-down behavior, thus making braking index determinations difficult, or that it may be a stable rotator over long periods of time between glitches (like the Crab pulsar) and that one of the two values, ~2 or ~2.8, is indicative of the long-term behavior.

In this article we report optical observations carried out at the 3.6 m telescope at La Silla during 1989 January, 1989 December, 1990 March, 1990 September, 1990 November, 1991 January, 1991 March, and 1991 April. In § 2 we describe the observations. Section 3 discusses the average pulse profile and intensity measurements for these data. The frequency measurements and a self-consistent ephemeris spanning the data set are presented in § 4. Finally, a discussion of the implications of the results is given in § 5.

2. OBSERVATIONS

PSR 0540−69 was observed for a total of 15 observing sessions between 1989 January and 1991 April with the 3.6 m telescope at ESO's La Silla Facility as part of a larger program to search for a pulsar in SN 1987A. Table 1 displays the observation start times (UTC) and durations of each observing session. The 3.6 m telescope was outfitted with a photometer consisting of a photomultiplier with a GaAs photocathode with a flat response between 0.35 and 0.90 μm connected to a photon counting system. The photometer was operated at a sampling frequency of 10 kHz, and the output of the photon counting system was recorded sequentially on magnetic tape after summing over the sample time. The absolute UTC was recorded at the beginning of each data run with an accuracy of 1 ms and the relative accuracy of the sampling frequency was $\leq 10^{-8}$. Depending on the background due to moonlight, the seeing and the weather conditions diaphragms of 4″–15″ were used. Guiding was assured by offsetting stars in the field of view. The coordinates used were those given by Seward et al. (1984). The observing strategy was to (*a*) observe the Crab pulsar for a short time in order to calibrate the photometer and provide a check for the timing procedures in the subsequent analysis, and (*b*) observe PSR 0540−69 for typically 2000–3000 s twice during each observing session; once early and, conditions permitting once late.

3. PULSE SHAPE AND INTENSITY VARIATIONS

The pulse profile of PSR 0540−69 can be characterized by a broad feature over half of a cycle of the 50 ms spin period. Superposed upon this broad feature is a double-peaked structure separated by ~0.2 in pulsar phase (Middleditch & Pennypacker 1985). We have measured the average pulse profile

TABLE 1

LOG OF OBSERVATIONS

Date (UTC)	Start (h m s)	Duration (s)	Diaphragm (″)
1989 Jan 14	4 42 00	3120	4
1989 Dec 8	6 25 30	2970	4
1990 Mar 6	0 34 30	1890	15
1990 Sep 29	4 33 11	1968	10
1990 Sep 29	9 22 58	900	10
1990 Nov 8	5 18 35	417	15
1990 Nov 8	5 28 15	2705	15
1991 Jan 9	1 48 15	2219	10
1991 Jan 9	8 14 12	1078	10
1991 Jan 10	1 37 35	2247	7
1991 Jan 10	5 36 45	2656	7
1991 Mar 22	1 23 27	3188	10
1991 Mar 23	0 28 00	3179	10
1991 Apr 8	0 11 04	3266	10
1991 Apr 11	0 42 40	3232	10

for the data from 1990 September, 1991 January, 1991 March and 1991 April listed in Table 1 in the following manner. For each of the 10 observations 50 bin phaseograms were accumulated using the frequencies listed in Table 2. To align the phaseograms the second observation of January 10 (see Table 2) was used as a reference. Each phaseogram was, in turn, compared to the reference on a bin-by-bin basis and the squared differences were calculated. The phaseogram was then shifted by one bin with respect to the reference and the squared differences calculated again. This procedure continued until the differences were minimized. The resulting phase-aligned pulse profiles were then added and normalized to unit area. The average pulse profile, displayed in Figure 1, exhibits the broad half-cycle enhancement and the double-peaked structure. The pulsed fraction is 0.25% $\pm$ 0.03%. The dominant contribution to the background level against which the pulsed fraction is measured is due to the night sky and the pulsars nebular component. To ascertain the stability of the pulse profile throughout the observations we have measured the variance of the individual bins of Figure 1. For each individual observation the average background, defined as the average of the pulse profile over phases 0.08–0.18, was subtracted from the profile. Each of the background-subtracted profiles was then normalized to unit area and the variance of each bin calculated. This normalization scheme was an attempt to eliminate the differences in gain and sensitivity during different nights. The results are shown in Figure 2. Within our alignment accuracy of 0.04 cycles, Figure 2 indicates that the pulse profile is constant in time.

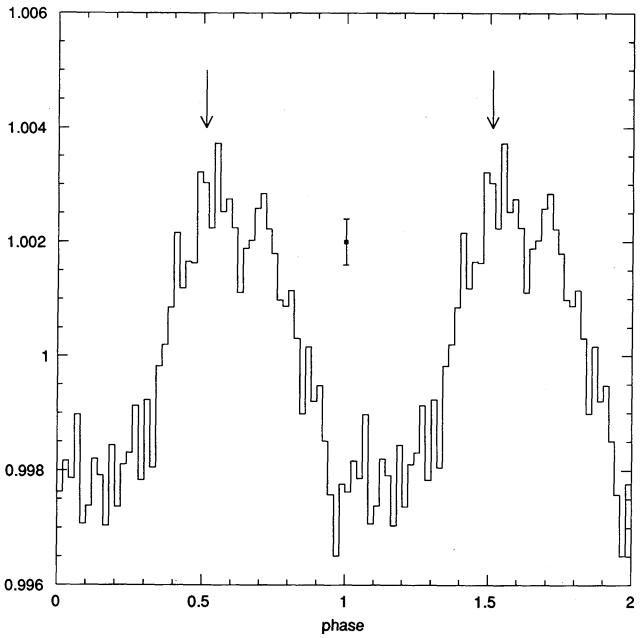

FIG. 1.—The average pulse profile for PSR 0540−69. The arrow indicates the reference phase for the quoted arrival times of Table 2 and the data point displays a typical error. The profile was normalized to unit area. Two cycles are plotted for clarity.

Although the sensitivity of every observation night has been calibrated once with the Crab pulsar's pulsed count rate, the changing conditions of seeing and transmission throughout the

TABLE 2

PULSE ARRIVAL TIMES FOR PSR 0540−69

UTC	Barycentric TOA TDB scale (JD-2,440,000)	Frequency (ν) Hz
1989 Jan 14	7540.7144[a]	19.86194(3)[b]
1989 Dec 8	7868.7860[a]	19.85658(3)
1990 Mar 6	7956.535347628	19.85518(4)
1990 Sep 29	8163.701905093	19.85172(7)
1990 Sep 29	8163.895228209	19.85175(40)
1990 Nov 8	8203.724220197	19.85089(30)
1990 Nov 8	8203.744171419	19.85114(3)
1991 Jan 9	8265.588365604	19.85015(2)
1991 Jan 9	8265.849783919	19.85022(10)
1991 Jan 10	8266.581119021	19.85013(2)
1991 Jan 10	8266.749572947	19.85012(1)
1991 Mar 22	8337.576902062	19.84896(2)
1991 Mar 23	8338.538351173	19.84894(3)
1991 Apr 8	8354.527177476	19.84868(3)
1991 Apr 11	8357.548946644	19.84864(2)

[a] Arrival times not used in the pulse timing analysis due to errors in determination of the absolute time.

[b] Numbers in parentheses are the 1 σ errors in the last quoted digit.

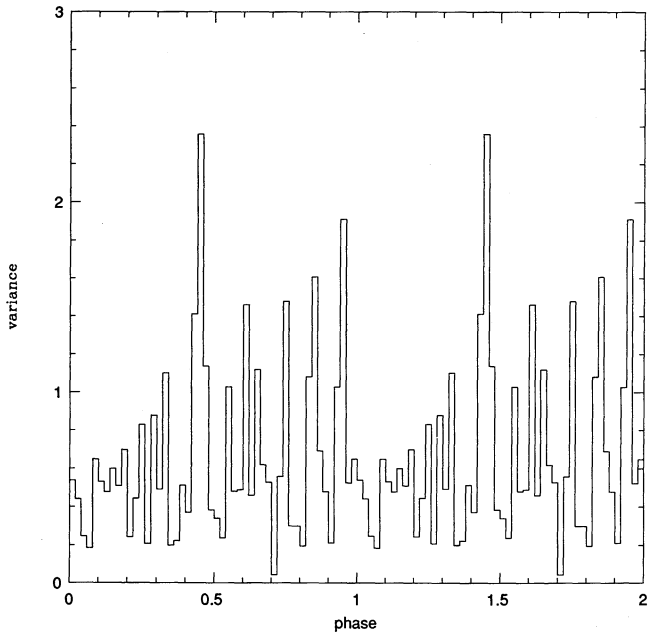

FIG. 2.—The variance of the bins in the pulse profile of PSR 0540−69. Two cycles of the 50 ms spin period are plotted for clarity.

night render our absolute flux measurements of PSR 0540−69 inaccurate. Nevertheless, we have determined the "pulsed" count rate of PSR 0540−69 with respect to the Crab pulsar using the calibration observations with the same diaphragm size. After determining the folded pulse shape of the Crab pulsar, the unpulsed background level was measured by averaging over the phase interval 0.15–0.20 phases prior to the main pulse peak. Subtraction of this rate from the average gave the pulsed count rate of the Crab pulsar. Using an average absorption coefficient of 0.2 mag per airmass for the no-filter response of the photomultiplier, the pulsed Crab pulsar and PSR 0540−69 rates were corrected to the top of the atmosphere. The average count rate of PSR 0540−69 thus determined was a factor 120 ± 10 times less than the Crab pulsar's where the error has been calculated from the variance of the measurements of each night. Assuming that the Crab pulsar's average flux density in the range of the photomultiplier (0.35–0.90 μm) is 850 μJy (Middleditch et al. 1987) implies that PSR 0540−69 has a flux density of 7.1 ± 0.6 μJy in the same wavelength range at the top of the atmosphere.

4. ROTATION FREQUENCY

The analysis of the rotational properties of PSR 0540−69 was done in four main steps consisting of (i) determination of the barycentric rotation frequency and time of arrival of the pulse (TOA) for each continuous data set; (ii) obtaining an improved rotation frequency for the data sets separated by few days or less by phase-relating the arrival times; (iii) using these improved rotation frequencies together with all our other optical measurements plus the *GINGA* (Nagase et al. 1990) and *ROSAT* (Ögelman, Hasinger, & Trümper 1991) data to fit a long-term quadratic trend to the frequency plus its first and second derivatives (ν_0, $\dot{\nu}_0$, $\ddot{\nu}$); (iv) using the time of arrivals of each continuous data set and the ephemeris derived in step (iii), determine a more accurate set of ν_0, $\dot{\nu}_0$, $\ddot{\nu}$. We describe the details of each step below.

In the first step, due to the broad pulse shape of PSR 0540−69, the raw data were summed over five samples to yield a 0.5 ms integration time. The arrival time of the center of each integration bin was propagated to the solar system barycenter using the JPL DE200 ephemeris. The adopted J2000.0 coordinates of PSR 0540−69 used for the barycentric correction were $\alpha = 5^h40^m11^s.03$, $\delta = -69°19'57''.5$. The best frequency for each observing run listed in Table 1 was determined by folding the barycentered times at the test frequency and calculating the Z_2^2 statistic (Buccheri et al. 1983). The TOA of the pulse was determined from the folded light curve using the first hump of the double-humped maximum (see the average pulse shape in Fig. 1). Although the folding was done using the barycentric UTC times, the TOAs were subsequently converted to barycentric dynamic time (TDB) by adding the TDB − UTC correction. As a check of the timing programs, observations of the Crab pulsar taken during the same observing sessions were analyzed in an identical fashion and the absolute phase of the radio main peak were checked against the Jodrell Bank ephemeris (Lyne & Pritchard 1991). We estimate the accuracy of the TOA measurements to 4% of a rotation period (~2 ms). Table 2 gives the frequency and TOAs determined for these data.

In the second step we obtained a new set of improved frequencies by phase relating self-consistently the relatively near TOAs and getting a frequency representing the epoch between the TOA measurements. These epochs (Julian Days) and frequencies (Hz) were respectively: 2,448,163.7986, 19.851798(3) (for 1990 September); 2,448,203.7342, 19.851077(40) (for 1990 November); 2,448,266.1919, 19.850130(1) (for 1991 January); 2,448,338.0571, 19.848957(1) (for 1991 March); and 2.448,356.0375, 19.8486635(3) (for 1991 April); parentheses are the estimated 1 σ errors in the last quoted digit.

In the third step, using the *GINGA* ephemeris (Nagase et al. 1990) plus the frequencies derived in the second step above, plus the optical results of 1989 January 14, 1989 December 8, 1990 March 6, plus the *ROSAT* data of 1990 June (Ögelman et al. 1991), we fitted a maximum likelihood least-squares quadratic curve to the frequencies obtaining the ephemeris listed in Table 3. The χ^2 per degree of freedom was less than 1, indicating a satisfactory fit.

In the fourth and final step we tried phase-relating all the TOAs listed in Table 1 using the ephemeris derived in the third step. We varied the pulse numbers associated with the TOAs until the phase residuals as well as the differences from ν_0, $\dot{\nu}_0$, $\ddot{\nu}$ derived in the third step were minimized. The pulse number assignments to the 12 TOA measurements covering the 1990 September to 1991 April interval were unique. However, the large gap between the 1990 March to 1990 September interval left a pulse number ambiguity of ±1. For the three possible solutions the rms value of the residuals was approximately 0.03 periods which is better than the estimated measurement error of ~0.04 periods. In all three solutions, the difference between ν_0, $\dot{\nu}_0$ derived in step 3 (*GINGA* plus *ROSAT* 1990 June plus ESO optical frequencies) and the phase-related fit of the optical data were about 2, and 8 σ, respectively at the epoch 1991 January 0. However, the $\ddot{\nu}$ of one pulse number choice (solution 1) was closer to the step 3 ephemeris (Table 3) than the other choices with one more pulse number difference (solutions 2 and 3) with differences of 2.6, 4.7, and 8.9 σ, respectively. Table 4 summarizes the ephemeris implied by each of the solutions. The residuals of the TOAs of solution 1, which we consider more likely since it gives a $\ddot{\nu}$ closer to the step 3 ephemeris, are displayed in Figure 3.

5. DISCUSSION

The fact that we were able to phase-relate the TOAs of the optical pulses over a span of about 420 days indicates that there were no large discontinuities in the rotational ephemeris of PSR 0540−69 during the interval 1990 March–1991 April. If we assume that PSR 0540−69 has the same type of timing noise as the Crab pulsar (phase or frequency noise), the upper limit to its "activity" (Cordes & Downs 1985), as deduced from the fit residuals, would be similar to that of the Crab pulsar.

TABLE 3

SPIN PARAMETERS FOR PSR 0540−69[a]

Parameter	Value
Epoch (JD TDB scale)	2,448,256.50000
ν_0 (Hz)	19.85028669(12)
$\dot{\nu}_0$ (10^{-10} Hz s^{-1})	−1.887556(12)
$\ddot{\nu}$ (10^{-21} Hz s^{-2})	3.79(2)
n (Braking index)	2.11(1)

[a] As a result of fitting the frequencies from *GINGA* + ESO + 1990 June *ROSAT* data to the form $\nu = \nu_0 + \dot{\nu}_0 t + 1/2\ddot{\nu}t^2$. Numbers in parentheses are the 1 σ errors in the last quoted digits.

TABLE 4

SPIN PARAMETERS FOR PSR 0540−69[a]

Parameter	Solution 1	Solution 2	Solution 3
Epoch (MJD TDB scale)	8256.500000127(23)	8256.500000127(23)	8256.500000128(23)
ν_0 (Hz)	19.850286413(3)	19.850286409(3)	19.850286416(3)
$\dot{\nu}_0$ (10^{-10} Hz s^{-1})	−1.887656(3)	−1.887658(3)	−1.887654(3)
$\ddot{\nu}$ (10^{-21} Hz s^{-2})	3.66(4)	4.02(4)	3.30(3)
n (Braking index)	2.04(2)	2.24(2)	1.84(1)

[a] As a result of fitting the phase-related ESO arrival times to the form $\phi = \phi_0 + \nu_0 t + \frac{1}{2}\dot{\nu}_0 t^2 + \frac{1}{6}\ddot{\nu} t^3$. Numbers in parentheses are the 1 σ errors in the last quoted digits. The epoch is the TOA in Julian Days (JD-2,440,000).

The measurements reported in this paper yield rotational parameters that confirm the continuation of the low braking index ($n = \nu\ddot{\nu}/\dot{\nu}^2 \simeq 2.0$) state measured by *GINGA* (Nagase et al. 1990), as opposed to the earlier braking index of $n \sim 2.7$ measured by Ögelman & Hasinger (1990). In fact, the solution 1 braking index of 2.04 ± 0.02 is, within errors, identical to the *GINGA* value of 2.02 ± 0.01; while solutions 2 and 3 have values of 2.24 ± 0.02 and 1.84 ± 0.01, respectively. It is this closeness of the braking index to the *GINGA* value that prejudices us to favor the solution 1 ephemeris derived in § 4.

It is interesting to compare the differences in the frequencies as determined by the *GINGA* and ESO ephemerides. In Figure 4 we show this difference for the three ESO solutions. Solutions 2 and 3 imply a discontinuity in the intervening interval between the *GINGA* and ESO measurements. In fact, solution 2 with a glitch of $\delta\nu/\nu \sim +3 \times 10^{-8}$ and $\delta\dot{\nu}/\dot{\nu} \sim -3 \times 10^{-5}$ sometime around JD 2,447,700 would be compatible with the two ephemerides. Solution 3 would imply a similar magnitude glitch but opposite in the signs of both $\delta\nu$ and $\delta\dot{\nu}$. Small discontinuities of this magnitude and sign in ν and $\dot{\nu}$ are common in many pulsars (Cordes & Downs 1985). In principle, deviations larger than ± 1 pulse number from our best solution, solution 1, are acceptable if one ignores the compatibility to the frequency fit derived in step 3 and uses just the acceptable χ^2 range of the ESO arrival times. However, these higher pulse number deviations imply larger and larger glitches between the *GINGA* and ESO data sets, effectively violating our step 3 fit assumption of a glitch-free period between the *GINGA* + ESO measurement. Solution 1 displays the smoothest joining of the two data sets. Within errors, the backward extrapolation of the frequency from the ESO ephemeris does meet the *GINGA* frequency. The ESO frequency at the given epoch is, however, $4.4 \pm 0.5 \times 10^{-7}$ Hz higher than the forward extrapolation of the *GINGA* frequency. This deviation is too large to be attributed to torque noise as it would require a frequency noise strength of $S_{FN} > 2 \times 10^{-21}$ Hz^2 s^{-1}, an order of magnitude larger than the noise strength estimated from the phase residuals of the fit of these data as well as from previous optical work of Manchester & Peterson (1989). Although it is possible to account for this discrepancy by again invoking a small discontinuity of $\delta\nu/\nu \sim +10^{-8}$ and $\delta\dot{\nu}/\dot{\nu} \sim +3 \times 10^{-5}$ around JD 2,447,700 it is interesting to consider the possibility of a $\ddot{\nu}$ term. A value of $\ddot{\nu} \sim 1.5 \pm 0.5 \times 10^{-30}$ Hz s^{-3} can reduce the discrepancy between the two ephemerides. This value of $\ddot{\nu}$ is about a factor of 2 larger than the value observed in the Crab pulsar and of opposite sign (Lyne, Pritchard, & Smith 1988). The existence of this term implies a growing braking index with a time scale $\tau_{B.I.} \simeq \ddot{\nu}/2\dot{\nu} \simeq 40$ yr. Such time scales may be indicative of changes in the surface field geometry or crustal

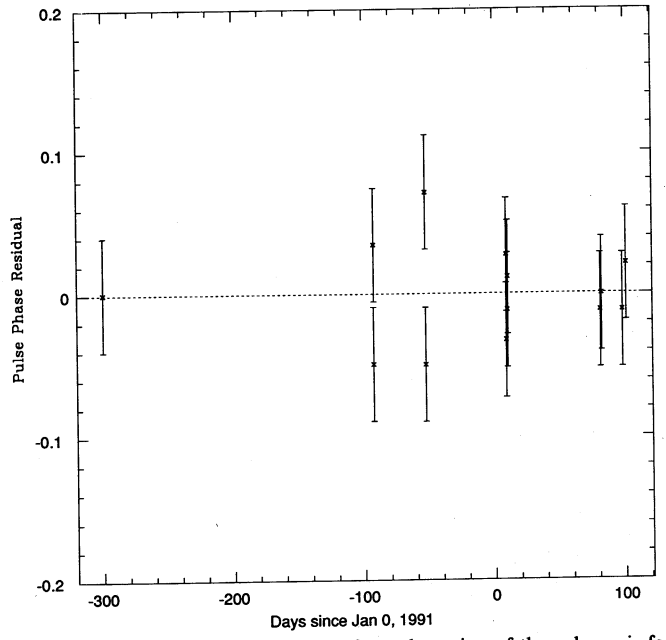

FIG. 3.—The pulse phase residuals after subtraction of the ephemeris for solution 1 given in Table 4.

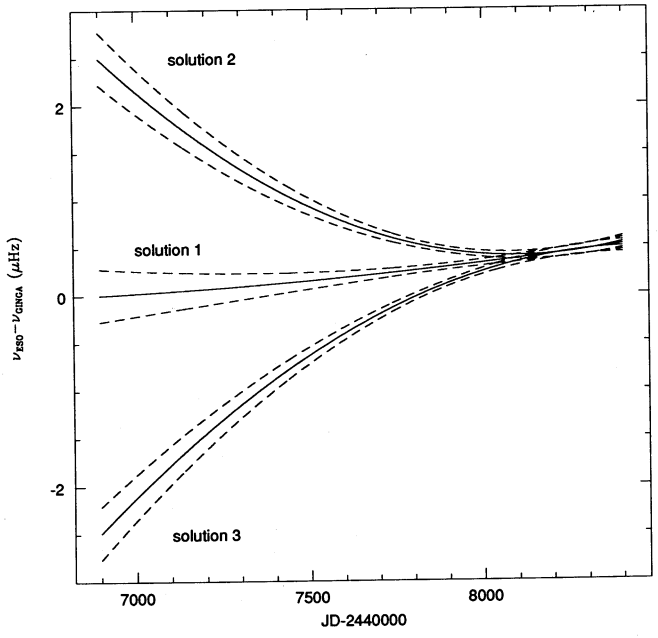

FIG. 4.—The frequency difference between the three possible ESO ephemerides of Table 4 and the published *GINGA* ephemeris (Nagase et al. 1990) as a function of time. The dashed lines are the 1 σ error limits on the difference.

structure of neutron stars (Blandford & Romani 1988; Alpar & Ögelman 1990). The accuracy of these results will improve with further observations of the rotational behavior of PSR 0540−69.

The authors gratefully acknowledge the support of the ESO technical staff at La Silla. We would also like to thank John Deeter and Paul Boynton for useful discussions. This work was supported in part by NASA grant NAGW-2643.

REFERENCES

Alpar, M. A., & Ögelman, H. 1990, ApJ, 349, L55
Blandford, R. D., & Romani, R. W. 1988, MNRAS, 234, 57P
Buccheri, R., et al. 1983, A&A, 128, 245
Cordes, J. M., & Downes, G. S. 1985, ApJS, 59, 343
Lyne, A. G., & Pritchard, R. S. 1991, private communication
Lyne., A. G., Pritchard, R. S., & Smith, F. G. 1988, MNRAS, 233, 667
Manchester, R. N., & Peterson, B. A. 1989, ApJ, 342, L23
Middleditch, J., & Pennypacker, C. R. 1985, Nature, 313, 659
Middleditch, J., Pennypacker, C. R., & Burns, M. S. 1987, ApJ, 315, 142
Nagase, F., Deeter, J., Lewis, W., Dotani, T., Makino, F., & Mitsuda, K. 1990, ApJ, 351, L13
Ögelman, H., & Hasinger, G. 1990, ApJ, 353, L21
Ögelman, H., Hasinger, G., & Trümper, J. 1991, IAU Circ., No. 5321
Seward, F. D., Harnden, F. R., Jr., & Helfand, D. J. 1984, ApJ, 287, L19